SCATTERING OF CHIRAL ELECTRONS BY CHIRAL MOLECULES

T.J. Gay, M.E. Johnston,[1] K.W. Trantham, and G.A. Gallup

Behlen Laboratory of Physics
University of Nebraska
Lincoln, Nebraska 68588-0111 U.S.A.

INTRODUCTION

In 1811, Arago demonstrated that when linearly-polarized light passes through a chiral medium, its plane of polarization is rotated. This experimental result, called *optical activity*, was analyzed by Fresnel in 1825, who showed that it was complementary to a second effect, *circular dichroism*, in which, e.g., left-handed circularly polarized light is scattered more strongly in a chiral medium than is light with right-handed circular polarization. Optically active substances that cause clockwise rotation of the polarization plane with respect to an observer looking at the light source are called *dextrorotatory*, or "right-handed." Substances that cause anti-clockwise rotations are *levorotatory*, or "left-handed." These phenomena have been well-characterized in the intervening years.[2] Since electrons, like photons, can be polarized,[3] it is interesting to speculate that similar phenomena might be observed in electron scattering from chiral targets. Such electronic analogs would be of physical significance in their own right, but would also have interesting implications for biophysics.

It is known that all naturally-occurring biological amino acids are left-handed, while organic sugars are right-handed. Since the primordial precursors of organic materials on earth were presumably synthesized electrochemically, and hence with initially equal numbers of left- and right-handed molecules, the mechanism whereby one chirality ultimately "won out" over the other has been the subject of much debate. One model,[4,5] often referred to as the "Vester-Ulbricht hypothesis of biological homochirality," postulates that beta-radiation, which is longitudinally polarized and hence chiral, preferentially destroyed right-handed

amino acids in the initially racemic primordial mixture. This idea led to a number of experiments designed to look for asymmetries in the interactions between longitudinally-polarized electrons or positrons and solid chiral biological targets. While some evidence has been found for such effects,[6] from the standpoint of basic physics it would be more interesting to observe them in electron scattering by single molecules, as opposed to bulk targets, so that there would be some hope of identifying specific chiral dynamical mechanisms responsible for the asymmetries.

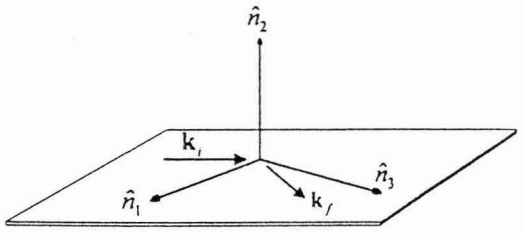

Figure 1. Collision coordinate system defined in equation 1.

In two pioneering papers published in the early 1980's, Farago discussed mathematically the symmetry principles relevant for observing electronic analogs of optical activity and circular dichroism in electron-molecule scattering.[7,8] His development is summarized here. Consider the simplest case of elastic scattering of non-relativistic electrons by a spinless target, in which the initial and final electron momenta, $\vec{k}_i$ and $\vec{k}_f$ respectively, are used to define a collisional coordinate system (figure 1):

$$\begin{aligned}
\hat{n}_1 &= \left(\vec{k}_f - \vec{k}_i\right) \Big/ \left|\left(\vec{k}_f - \vec{k}_i\right)\right|, \\
\hat{n}_2 &= \left(\vec{k}_i \times \vec{k}_f\right) \Big/ \left|\left(\vec{k}_f \times \vec{k}_i\right)\right|, \text{ and} \\
\hat{n}_3 &= \left(\vec{k}_i + \vec{k}_f\right) \Big/ \left|\left(\vec{k}_i + \vec{k}_f\right)\right|.
\end{aligned} \tag{1}$$

In this case, the final-state spin density matrix ρ_f can be defined in terms of a spin scattering matrix M and the initial density matrix ρ_i:

$$\rho_f = M \rho_i M^{\dagger}. \tag{2}$$

The scattering matrix can, in turn, be expanded in terms of the Pauli spin matrices, the unit matrix, and a series of amplitudes that are implicitly dependent on $\vec{k}_i$ and $\vec{k}_f$:

$$M = f\sigma_o + f'\vec{\sigma}\cdot\hat{n}_1 + g\vec{\sigma}\cdot\hat{n}_2 + h\vec{\sigma}\cdot\hat{n}_3, \tag{3}$$

where

$$\vec{\sigma}\cdot\hat{n}_1 = \begin{pmatrix} 0 & 1 \\ 1 & 0 \end{pmatrix}, \ \vec{\sigma}\cdot\hat{n}_2 = \begin{pmatrix} 0 & -i \\ i & 0 \end{pmatrix}, \ \vec{\sigma}\cdot\hat{n}_3 = \begin{pmatrix} 1 & 0 \\ 0 & -1 \end{pmatrix}, \tag{4}$$

and σ_o is the 2×2 unit matrix. We now assume that the scattering interaction is invariant under the operation of spatial rotations, time-reversal, and inversion (parity). This means that under the action of a given symmetry operator, each term of M must remain invariant, or be

identically zero. This is manifestly true for spatial rotations. Under time reversal, however, $\vec{\sigma}$ flips sign, as do $\hat{n}_2$ and $\hat{n}_3$. Thus while the first, third, and fourth terms of eq.3 remain the same under time reversal, the second flips its sign, meaning that f' must be zero. Finally, we note that $\hat{n}_2$ is an axial vector, whereas $\hat{n}_3$ is polar. The three components of $\vec{\sigma}$ are axial vectors. Thus under inversion $\vec{\sigma}\cdot\hat{n}_2$ will not change sign but $\vec{\sigma}\cdot\hat{n}_3$ will. Therefore h must be identically zero *unless* it also flips sign under inversion. This can happen only if the target is chiral, i.e., lacks any element of symmetry that is an improper rotation. Target chirality, in turn, can be the result of electroweak interactions (which we neglect), spatial orientation (which we do not consider), or of the stereochemical arrangement of the atoms making up the molecule itself. At least four atoms in a non-planar geometry are required for a molecule to be chiral.

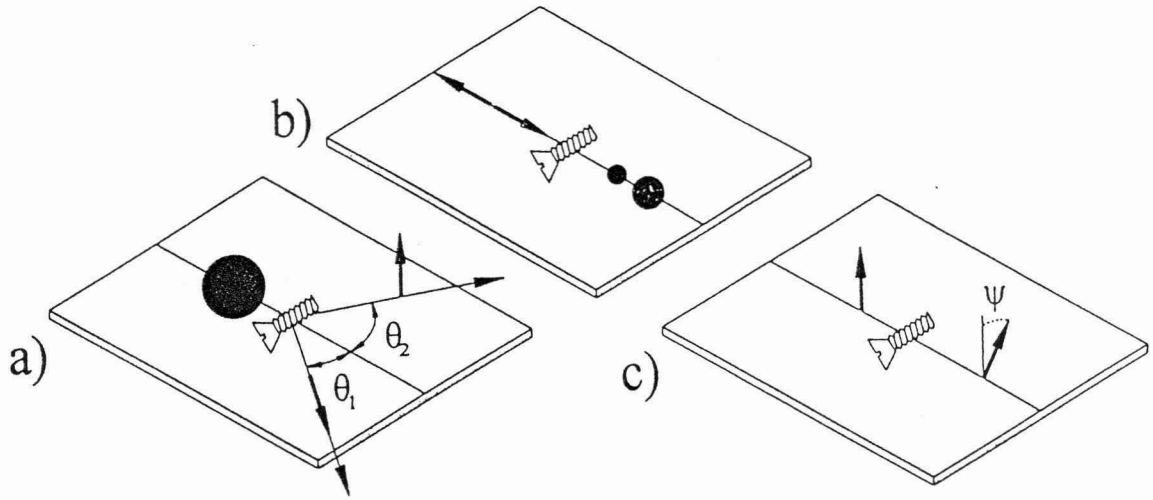

Figure 2. Chiral effects in electron-molecule scattering (see text). a) Production of in-plane polarization of electrons scattered to Θ_1. Transverse polarization production (electrons scattered to Θ_2) does not require chiral targets. b) Preferential transmission of electrons with a given helicity. c) Rotation of initially transverse polarization about the incident momentum.

Farago discussed three classes of "parity-violating," or chiral effects, illustrated schematically in figure 2. Each requires that the amplitude h be non-zero.

(1) Production of polarization of the scattered beam in the plane of scattering. If the incident beam of unit intensity is unpolarized, the scattered flux at (θ,ϕ) is given by

$$I(\theta,\phi) = |f(\theta,\phi)|^2 + |g(\theta,\phi)|^2 + |h(\theta,\phi)|^2, \tag{5}$$

and its polarization components along the three unit vectors are

$$\begin{aligned} \vec{P}\cdot\hat{n}_1 &= \frac{1}{2I}\left(|g+ih|^2 - |g-ih|^2\right), \\ \vec{P}\cdot\hat{n}_2 &= \frac{1}{2I}\left(|f+g|^2 - |f-g|^2\right), \text{ and} \\ \vec{P}\cdot\hat{n}_3 &= \frac{1}{2I}\left(|f+h|^2 - |f-h|^2\right). \end{aligned} \tag{6}$$

The polarization along $\hat{n}_2$ is independent of the chiral amplitude h, and corresponds simply to

Mott scattering, i.e. the production of polarization by spin-orbit coupling between the continuum electron and one (or perhaps more) of the target nuclei. The remaining two polarization components are in the plane of scattering; they will be present only if the chiral scattering amplitude is non-zero. Notice that the magnitude of these components depends on cross terms involving either gh or fh, so that parity-violating effects will be reduced generally by simple ratios of the parity-violating and non-parity-violating amplitudes, as opposed to the ratios of their squares.

(2) Rotation of incident transverse polarization. For incident electrons that are transversely polarized and that are scattered into the forward direction ($\theta=0^0$), the initial polarization vector can be rotated in the plane perpendicular to $\bar{k}_i$ by an angle

$$\psi = \frac{4\pi\lambda}{k} dz\, Re(h), \tag{7}$$

where $k=k_i=k_f$, λ is the target's areal density, and dz is the path length of the electron beam through the target. This effect is thus analogous to optical activity; in that case the rotation angle is also proportional to target thickness and the real part of the optical index of refraction.

(3) Polarization-dependent beam attenuation. Consider now an incident beam with longitudinal polarization either parallel or anti-parallel to its momentum (i.e. with positive or negative helicity). In analogy with photon circular dichroism, a chiral target will preferentially attenuate one helicity over the other. The attenuation asymmetry, A, is given by

$$A = \frac{I^+ - I^-}{I^+ - I^-} = -P_e \frac{4\pi\lambda}{k} dz\, Im\,(h), \tag{8}$$

where $I^{\pm}$ is the intensity of electrons with positive or negative helicity exiting the target undeflected (scattered to 0°), and P_e is the beam's initial longitudinal polarization. The formula for optical circular dichroism is essentially identical to this, involving the imaginary part of the index of refraction.

For chiral targets, the effects listed above are permitted on the basis of symmetry considerations alone. But it is instructive to consider the dynamical mechanisms that cause these effects, i.e. that yield a non-zero value for h. To do this, we consider the specific case of production of longitudinal polarization in the scattered beam. There are essentially three clearly distinguishable mechanisms, which we have illustrated schematically in figure 3. The first was proposed by Kessler[9] in 1982 (fig.3a), and involves a combination of Mott scattering followed by plural electrostatic scattering. For the molecular orientation shown, the incident unpolarized beam is scattered from a first atom. Because of the spin-orbit interaction between the continuum electron and the atomic nucleus, a transverse polarization is generated in the first (Mott) scattering. Neglecting any further spin-orbit coupling, a second, purely electrostatic scattering now deflects the electron to its final path without affecting its spin. Thus the intermediate transverse polarization is partially converted to longitudinal polarization. This scattering sequence could of course happen with a non-chiral target with this specific orientation. But it is only with chiral targets that an average of the longitudinal polarization over all target orientations is not reduced to zero. These

considerations imply that chiral effects will be biggest if there is an atom with high Z (to enhance the spin-orbit coupling) located at or near the molecule's chiral center.

A second mechanism, involving induced electric and magnetic moments in the target, is analogous to that responsible for chiral optical effects[2], and has been discussed by Walker[10] and Gallup[11] (fig.3b). We consider again a specific orientation of the chiral target and outgoing electron trajectory. As the incident electron approaches the molecule, it induces a time-varying electric dipole moment on the target. Because of the molecule's chirality, this electric moment causes a net orbital angular momentum of the target electrons, yielding a magnetic dipole. This dipole in turn interacts with the incident electron spin, yielding a "spin-other-orbit" term in the scattering Hamiltonian. The sign of this term, and the resultant differential scattering cross section, depends on whether the incident electron helicity is positive or negative; i.e. the probability of an electron being scattered to a specific angle will depend on its initial spin. The scattering process thus acts as a "spin filter," and yields a longitudinal polarization of the scattered beam. In this model we neglect spin-flip processes. The important quantities for determining the magnitude of the expected effects are the electric and magnetic polarizabilities; individual nuclear charges are important only to the extent that there is a correlation between nuclear charge and atomic size, and hence polarizability. This offers the possibility that the judicious choice of a series of targets could allow a determination of the relative importance of mechanisms one and two.

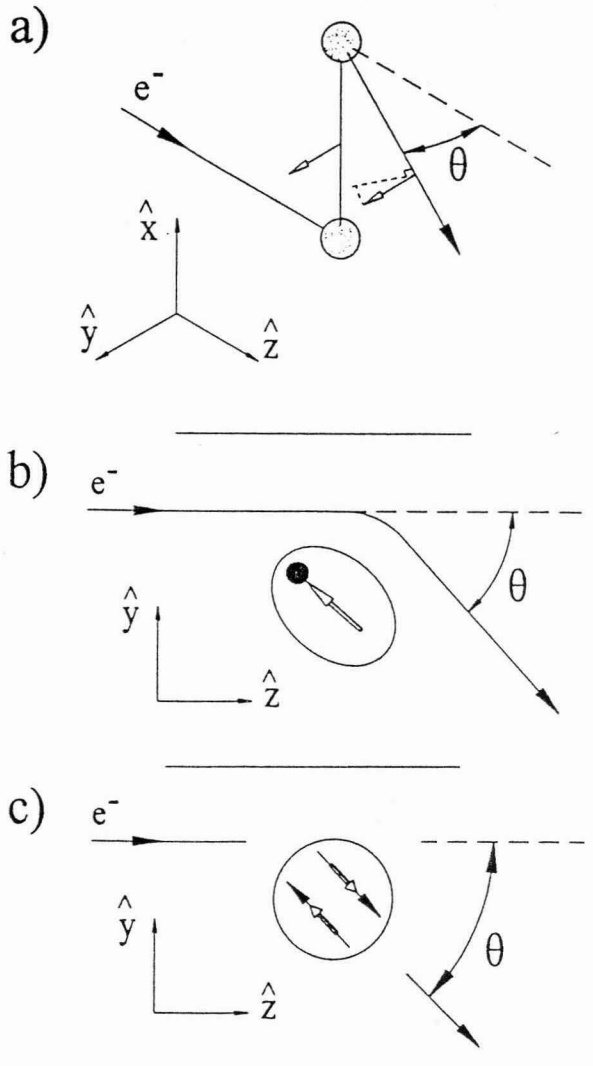

Figure 3. Dynamical causes of chiral scattering effects (see text).

A final mechanism invokes the concept of the target's "helicity density," an idea developed by Hegstrom, Rich, and coworkers.[12,13] In a closed-shell chiral target with a high-Z atom near the chiral center, the singlet and triplet character of the molecular wave functions are partially lost due to the spin-orbit coupling with the high-Z nucleus. This spin mixing results in a non-zero local expectation value of the helicity operator

$$\bar{H} = \hbar^{-1}\bar{\sigma}\cdot\bar{\nabla}; \qquad (9)$$

in these regions there is a correlation between an electron's momentum and its spin. Thus for the target as a whole, there is a net electron helicity, i.e. on average the electrons of the target will be spinning in (for example) the same direction they are moving. While the helicity density can be non-zero locally in achiral molecules (around any local chiral center), the net helicity, integrated over the entire molecular electron density, must be zero. The helicity density of the chiral molecule camphor is shown in figure 4.

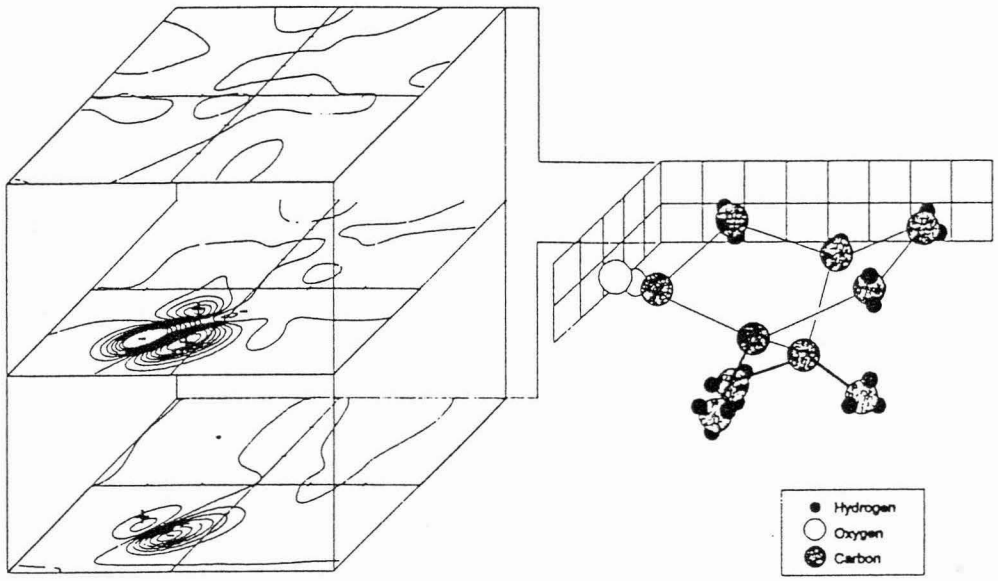

Figure 4. Helicity density in three cross sections of the (right-handed) camphor molecule.

We consider again scattering to a specific angle (fig. 3c), but now that a net helicity of the target has been assumed, we need not posit a given target orientation. The scattered electrons will have originated either in the incident beam ("direct" scattering) or the target ("exchange" scattering). Now it will be generally true that for exchange scattering there will be a dynamical preference for electrons initially on the target whose momenta during the scattering process are parallel (or *vice versa*) to the final momentum vector selected by the scattering experiment. The component of the scattered beam due to direct processes will be unpolarized, but the exchange component will have a longitudinal polarization reflecting this dynamical preference in conjunction with the target's net helicity.

In 1981, Beerlage *et al.*[14] reported a search for longitudinal polarization in initially unpolarized electrons scattered by a camphor target. At an incident energy of 25 eV, at scattering angles between 40° and 70°, their results were consistent with zero to a precision of 5×10^{-3}. But in 1985, Campbell and Farago[15,16] reported a non-zero scattering asymmetry when they measured the current of 28% longitudinally-polarized 5eV electrons transmitted through a target of camphor vapor. Their values of A (eq.8) were $50(17)\times10^{-4}$ for right-handed camphor and $-23(11)\times10^{-4}$ for left-handed camphor. We note that the left- and right-handed results have opposite sign, as they must, and that when the absolute values of the two results are combined, they yield a result more than three standard deviations away from zero: $31(9)\times10^{-4}$. This result was both important and surprising, offering as it did the first evidence of an electronic analog of circular dichroism, and in a molecular target, as opposed to the bulk, where some hope could be held for a good understanding of the origins of the

In this experiment, we measured electron polarizations ranging from 26% for bulk GaAs crystals to 47% for epitaxially-grown GaAs.

The electron beam was transported at 200 eV into the camphor target chamber, shown schematically in figure 5. The chamber has a cylindrical glass vacuum housing that is concentric with the electron optical system. This lens system was used to decelerate the beam to its collision energy between 0.9 and 10 eV. The camphor collision cell was fed by a heated vapor line, and the vapor pressure in the cell was monitored by a capacitance manometer. Immediately downstream from the target is a retarding field analyzer (RFA), followed by an electron multiplier. In this experiment, we used devices with both discrete and continuous dynodes. The RFA and the aperture immediately succeeding it served to make cuts in energy and angle on the transmitted electrons. Campbell and Farago's experiment detected electrons that had not suffered angular deviations greater than 2° or energy losses greater than 200 meV. Using the program SIMION[23] to model the axially symmetric RFA and its exit aperture, we calculated the appropriate aperture diameter and electrode voltages necessary to ensure similar conditions with our apparatus, assuming the worst case of isotropic scattering. The resulting electron transmission histogram for one set of parameters is shown in figure 6. Subsequent RFA spectra taken with the apparatus agreed well with our model calculations.

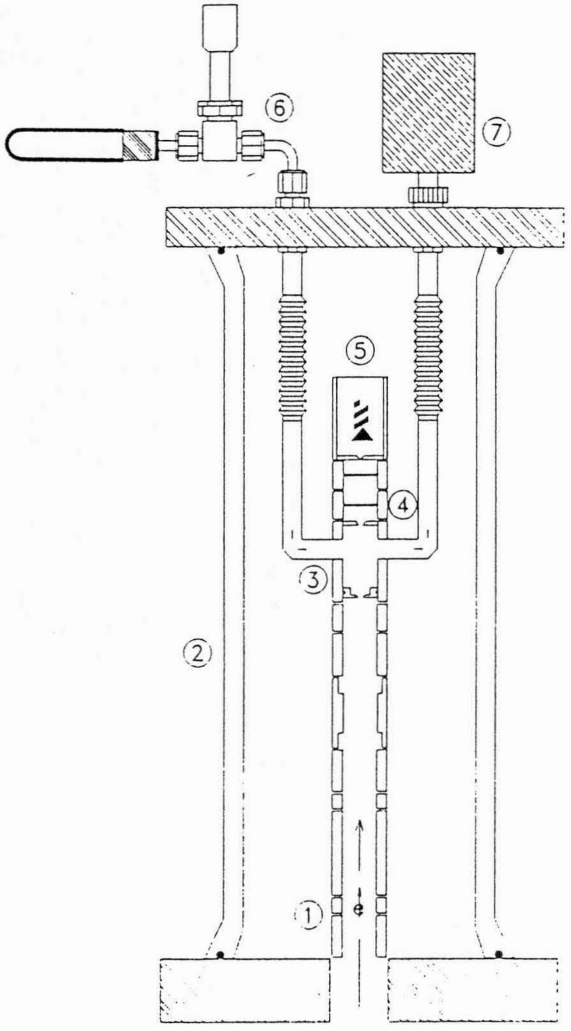

Figure 5. Camphor target chamber showing 1) input electron lenses; 2) glass vacuum chamber; 3) camphor target cell; 4) post-collision retarding field analyzer; 5) electron multiplier; 6) camphor reservoir system; and 7) capacitance manometer.

Camphor can cause problems when used as a target in low-energy electron scattering experiments. The most pernicious of these is changing electron-beam tuning characteristics and energies as camphor coats various electron-optical elements. Two other concerns in this experiment were poisoning of the GaAs crystal and a reduction of the detection efficiency of the electron multipliers used to monitor the transmitted electrons. In order to minimize the effusion of camphor vapor into the rest of the apparatus, the entrance and exit apertures of the target cell were of small diameter; 1.6 and 2.0 mm respectively. Another precaution we took was to heat the internal components of the target chamber to about 50°C through the glass

vacuum wall with infrared incandescent lamps. These measures were helpful but did not eliminate all problems. The GaAs photocathode activation lifetimes, which were effectively infinite with no camphor in the target cell, were at most 12h during data runs. This was true in spite of the fact that the GaAs was "two vacuum chambers away" from the target. A

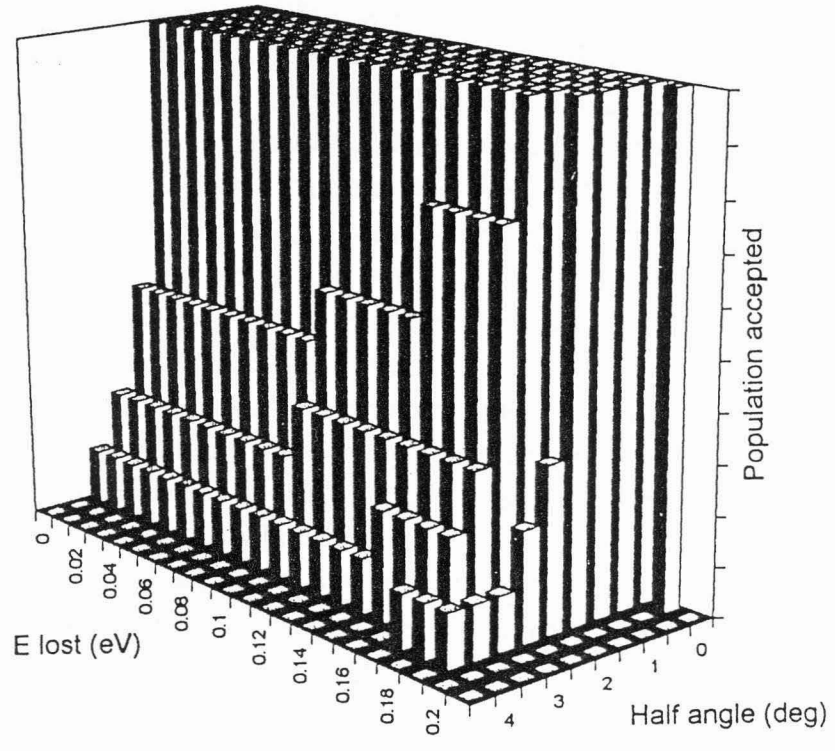

Figure 6. SIMION analysis[23] of electrons scattered in the target cell and subsequently detected (see text).

second, more serious problem was the contamination of the electron multipliers we used. At typical camphor operating pressures, we found the channel electron multipliers to have useful detection lifetimes between 36 and 100h. This led us to try "active film" discrete-dynode electron multipliers, but these devices exhibited even shorter lifetimes. On the other hand, they could be operated at much higher count rates. A possible remedy for the contamination problem would have been to bend the transmitted beam away from the target axis into the detectors, but we were reluctant to do anything to reduce our apparatus' axial symmetry.

DATA ACQUISITION PROTOCOL

Data taking proceeded in the following fashion. The electron beam from a freshly activated crystal was guided into the polarimeter where P_e was measured. With no camphor in the target cell, the beam was then directed onto the electron detector, after being defocussed so that the maximum permissible count rate of the electron multiplier was not exceeded. (This was about 50 kHz for the channeltrons and 1.5 MHz for the discrete dynode multipliers.[24]) At this point, camphor was admitted to the target cell until the incident beam had been attenuated by a factor of two. This required a target pressure of approximately 1 mTorr. After camphor had been in the target cell for a long enough time that the electron-

beam tuning potentials had equilibrated, the collision energy was set by adjusting the potential on the scattering cell, and comparing it with that required to completely block the incident beam. Then the RFA potential required to pass only electrons that had lost less than 0.2 eV was determined by taking a complete RFA spectrum.

A typical data-taking sequence for a given target chirality involved ~4 sets of 25 +/– electron helicity pairs. Data was taken for 2s with each helicity; the first helicity was selected randomly by computer. After a 4-set run, the target handedness was changed automatically. This was accomplished with a target handling system that had heated reservoirs of both antipodes of camphor. These reservoirs were connected to the target cell and to a dedicated vacuum line by means of heated stainless steel pipes and solenoid-controlled valves. After four more sets of data were collected with the other enantiomorph, the target helicity was toggled back and another group of data was acquired. This process was repeated until ~400 helicity pairs were accumulated for each handedness of camphor. A histogram of the individual asymmetries for each target chirality was then constructed. We found that while these histograms were Gaussian distributions, the standard deviations of the mean that characterized them were usually larger than would be expected on the basis of counting statistics alone. In all cases, we have therefore used the larger standard deviations of the mean for our quoted uncertainty limits.

The average of the two data sets of opposite handedness at a given incident energy was usually not zero to within our statistical uncertainty. This offset, which was reproducible and slightly energy-dependent, was taken to be a measure of our instrumental asymmetry. The offset values were consistent with instrumental asymmetries we measured using argon as a target.

Table 1. Camphor Asymmetries.

	Electron Energy (eV)	A (left) $\times 10^{-4}$	A (right) $\times 10^{-4}$	[A(right) – A(left)]/2 $\times 10^{-4}$
This work	1.0	–2(5)	+2(5)	2(4)
	3.0	0(5)	0(5)	0(4)
	5.0	–1(4)	+1(5)	+1(3)
	7.0	+3(6)	–3(6)	–3(4)
	10.0	0(2)	+1(7)	+1(4)
Ref. 16	5.0	–178(61)	82(39)	260(36)

RESULTS

The values of A we measured (eq.1) as a function of incident electron energy are given in Table 1. These results have been normalized to the electron polarization, and are compared with the results of Campbell and Farago, normalized to their quoted value of P_e: 28%. It is apparent that we have failed to reproduce Campbell and Farago's results. Our values of A are more consistent with the theoretical upper limits on chiral effects discussed previously. It is disappointing that we found no evidence for non-zero asymmetries, even at the lowest

energy, 1eV, where a strong negative ion resonance has been shown to exist.[20]

Another article in this volume discusses evidence for non-zero chiral effects in a ytterbium-based compound[25], and confirms our result in camphor. The next experimental challenge in this area will be to choose targets that elucidate which of the dynamical mechanisms discussed above is responsible for these effects.

ACKNOWLEDGEMENTS

The authors would like to thank P.D. Burrow for numerous useful discussions. This work was supported by the University of Missouri, the University of Nebraska, and by the National Science Foundation (Grant # PHY-9504350).

REFERENCES

1. Permanent address: Physics Department, University of St. Thomas, St. Paul, MN 55105-1096.
2. L.D. Barron. "Molecular Light Scattering and Optical Activity," Cambridge University Press, Cambridge (1982).
3. J. Kessler. "Polarized Electrons," 2nd ed., Springer, Berlin (1985).
4. S.L. Miller and L.E. Orgel. "The Origins of Life on the Earth," Prentice-Hall, Englewood Cliffs (1974).
5. D.C. Walker (editor). "Origins of Optical Activity in Nature," Elsevier, Amsterdam (1979).
6. A.S. Garay and J.A. Ahlgren-Beckendorf, Differential interaction of chiral β-particles with enantiomers, *Nature* 346:451(1990), and references therein.
7. P.S. Farago, Spin-dependent features of electron scattering from optically active molecules, *J.Phys.B* 13:L567(1980).
8. P.S. Farago, Electron optic dichroism and electron optical activity, *J.Phys.B* 14:L743(1981).
9. J. Kessler, Polarisation components violating reflection symmetry in electron scattering from optically active molecules, *J.Phys.B* 15:L101(1982).
10. D.W. Walker, Electron scattering from optically active molecules, *J.Phys.B* 15:L289(1982).
11. G.A. Gallup, The scattering of longitudinally polarized electrons from chiral molecules and optical rotatory power, *in*: "Electron Collisions with Molecules, Clusters, and Surfaces," H. Ehrhardt and L.A. Morgan, eds., Plenum, New York (1994).
12. A. Rich, J. Van House, and R.A. Hegstrom, Calculation of a mirror asymmetric effect in electron scattering from chiral targets, *Phys.Rev.Lett.* 48:1341(1982).
13. R.A. Hegstrom, β decay and the origins chirality: theoretical results, *Nature* 297:643(1982).
14. M.J.M. Beerlage, P.S. Farago, and M.J. Van der Wiel, A search for spin effects in low-energy electron scattering from optically active camphor, *J.Phys.B* 14:3245(1981).
15. D.M. Campbell and P.S. Farago, Spin-dependent electron scattering from optically active molecules, *Nature*, 258:419(1985).
16. D.M. Campbell and P.S. Farago, Electron optic dichroism in camphor, *J.Phys.B* 20:5133(1987).

17. S. Hayashi, Asymmetry in elastic scattering of polarized electrons by optically active molecules, *J.Phys.B* 21:1037(1988).
18. R. Fandreyer, D. Thompson, and K. Blum, Attenuation of longitudinally polarized electron beams by chiral molecules, *J.Phys.B* 23:3031(1990).
19. K. Blum, Chiral effects in elastic electron-molecule collisions, these proceedings.
20. T.M. Stephen, X. Shi, and P.D. Burrow, Temporary negative-ion states of chiral molecules: camphor and 3-methylcyclopentanone, *J.Phys.B* 21:L169(1988).
21. J.E. Furst, W.M.K.P. Wijayaratna, D.H. Madison, and T.J. Gay, Investigation of spin-orbit effects in the excitation of noble gases by spin-polarized electrons, *Phys.Rev.A* 47:3775(1993).
22. T.J. Gay, J.E. Furst, K.W. Trantham, and W.M.K.P. Wijayaratna, Optical electron polarimetry with heavy noble gases, submitted to *Phys. Rev. A.*
23. SIMION is available from D.A. Dahl, Idaho National Engineering Laboratory, Idaho Falls, ID 83415.
24. K.W. Trantham, A count-rate safety circuit for high-voltage single-particle detectors, *Rev.Sci.Instrum.*, in press, to appear in November 1995.
25. S. Mayer and J. Kessler, Experimental study of spin-dependent electron scattering from chiral molecules, these proceedings.